Worst-Case and Distributional Robustness Analysis of Finite-Time Control Trajectories for Nonlinear Distributed Parameter Systems

Zoltán K. Nagy and Richard D. Braatz

***Abstract*—A novel approach is proposed that quantifies the influence of parameter and control implementation uncertainties upon the states and outputs of finite-time control trajectories for nonlinear lumped and distributed parameter systems. The worst-case values of the states and outputs due to model parameter uncertainties are computed as a function of time along the control trajectories. The algorithm can also compute the part of the optimal control trajectory for which implementation inaccuracies are of increased importance. An analytical expression is derived that provides an estimate of the distribution of the states and outputs as a function of time, based on simulation results. The approaches require a relatively low computational burden to perform the analysis, compared to Monte Carlo approaches for robustness analysis. The technique is applied to the crystallization of an inorganic chemical with uncertainties in the nucleation and growth parameters and in the implementation of the control trajectory.**

***Index Terms*—Crystallization, distributed parameter systems, optimal control, probabilistic analysis, robustness analysis, worst-case analysis.**

I. Introduction

MODEL-BASED process control has become important during the last few decades. It is attractive to use first-principles models, which are globally valid and, therefore, well suited for optimization that can require extrapolation beyond the range of data used to fit the model. However, it is impossible to generate highly accurate phenomenological models for most chemical processes because of inaccurate values for the physical parameters of the process, and lack of complete understanding of the underlying physical phenomena. The usually limited quality and quantity of input–output data used to fit the model ensures that the model will not be an exact representation of the true process. Thus, the practical implementation of model based simulation results often leads to a significant discrepancy between reality and simulation, whether the model is used for controller design or process optimization.

Manuscript received March 28, 2002. Manuscript received in final form August 6, 2002. Recommended by Associate Editor Ogunnaike. This work was supported in part by an NSF-NATO Postdoctoral Fellowship under NSF/DGE Award 0108053.

Z. K. Nagy was with the "Babes-Bolyai" University of Cluj, 3400 Cluj-Napoca, Romania (e-mail: znagy@chem.ubbcluj.ro). He is now with the University of Illinois at Urbana-Champaign, Urbana, IL 61801-3792 USA (e-mail: znagy@uiuc.edu).

R. D. Braatz is with the University of Illinois at Urbana-Champaign, Urbana, IL 61801-3792 USA (e-mail: braatz@uiuc.edu).

Digital Object Identifier 10.1109/TCST.2003.816419

The model-based computation of optimal control policies for batch and semibatch processes is of increasing interest due to industrial interest in improving productivity [2], [6], [17], [40]. However it has been shown that all of the benefits of using optimal control can be lost with subtle variation in either the model parameters or in the performance of the feedback controller to track the optimal setpoint trajectory [16], [41], [44]. This motivates the development of techniques to quantify the influence of parameter and control implementation uncertainties on the process states and outputs. Quantitative estimates obtained from robustness analysis can be used to decide whether more laboratory experiments are needed to provide better parameter estimates, or the design of an advanced control technique is necessary to ensure more accurate setpoint tracking [27], [34], [42].

The importance of taking model and control implementation uncertainty into account during the control design procedure has been well established [7], [21], [30], [39], [48], [49], [51]. An analysis tool has been developed to compute the worst-case deviation in the product quality for nonlinear lumped and distributed parameter systems due to uncertainties described by general Hölder norms [33], [35], [36]. Hölder norms are general enough to describe both ellipsoidal and infinity-norm uncertainty descriptions [33]. These studies considered the analysis of performance indexes at the end of the batch. However, most nonlinear model-based controllers require state feedback at every sampling instance during the batch. The performance obtained by implementing an optimal control policy strongly depends on how the states are influenced at intermediate time instances by model parameter uncertainty. The main contribution of this paper is the development of an approach for computing the worst-case values of the states and outputs due to the effects of model parameter uncertainties. The procedure applies to nonlinear lumped and distributed parameter systems that operate over finite time, which includes batch and semibatch processes. The procedure is extended to determine the period of the batch for which control implementation uncertainties have the strongest influence on the final product properties. This robustness analysis with regard to control implementation uncertainties can guide the selection of the control instrumentation, by determining where high precision sensing and actuation are required or a more advanced control algorithm has to be implemented. This paper applies the technique to compute the worst-case values for the state and outputs for the batch crystallization of an inorganic chemical subject to uncertainties in the nucleation and growth kinetics, and to control implementation uncertainties.

II. Problem Formulation and Solution

The main objective of the proposed approach is to compute the worst-case values for y (which can be any state or explicit function of the states) that can occur for a bounded set of uncertainties in the model parameters θ and the control trajectory u, and to analyze the evolution of these changes over time. A series expansion is used to describe y in the neighborhood around the control trajectory. The series expansion only needs to be accurate for the operating region defined by the nominal control trajectory and the parameter and implementation uncertainty description. Thus, the use of a low number of terms in the expansion can lead to satisfactory results, even for highly nonlinear processes [34]. After a worst-case analysis is completed, the accuracy of the results is evaluated by comparing the worst-case estimates with those obtained by a nonlinear dynamic simulation using the predicted worst-case model parameters and control trajectory. If the results are not sufficiently accurate, then a higher order series expansion is used, and the worst-case analysis is redone. This process is repeated until convergence. For all applications to date, only up to second-order expansions have been necessary to obtain high accuracy.

In the first-order case, this paper will also show how the distribution can be computed as an analytic function of the model simulation results.

A. Uncertainty Description

Define $\hat{\theta}$ as the nominal model parameter vector of dimension $(n \times 1)$, and $\delta\theta$ as the perturbation about $\hat{\theta}$. Then, the model parameter vector for the real system is

$$\theta = \hat{\theta} + \delta\theta. \tag{1}$$

Since we are interested in control algorithms that are implemented digitally, the nominal control trajectory can be represented as a vector $\hat{u}$ of dimension $(m \times 1)$. For example, a convenient representation for $\hat{u}$ in the case of a temperature trajectory defined over fixed range of time could be the temperatures at m discrete-time instances along the trajectory. Define δu as the perturbation about the nominal vector $\hat{u}$. Then, the control trajectory is

$$u = \hat{u} + \delta u. \tag{2}$$

It is desirable to define an uncertainty representation that is general enough to include the uncertainty descriptions common in practice. This can be done using the Hölder p-norm [28] defined for a general vector x by

$$\|x\|_p = \left(|x_1|^p + \cdots + |x_i|^p + \cdots + |x_n|^p\right)^{1/p} \quad p \geq 1 \tag{3}$$

$$\|x\|_\infty = \max_i |x_i|. \tag{4}$$

This description is general enough to include a hyper-ellipsoid on the model parameters described by [32]

$$\varepsilon_\theta = \left\{\theta: \left(\theta - \hat{\theta}\right)^T \mathbf{V}_\theta^{-1} \left(\theta - \hat{\theta}\right) \leq r^2(\alpha)\right\} \tag{5}$$

where

- $\mathbf{V}_\theta$ $(n \times n)$ positive definite covariance matrix;
- α confidence level, which is defined as the probability, based on a set of measurements, that the actual probability of an event is better than some specified level;
- r distribution function.

On the other hand, it is often convenient to describe control implementation uncertainties in terms of independent bounds on each element:

$$u_{\min,i} \leq u_i \leq u_{\max,i}, \quad i = 1, \ldots, m. \tag{6}$$

Using Hölder norms, the sets of parameters and control trajectories including uncertainties can be represented as

$$\varepsilon_\theta = \{\theta: \theta = \hat{\theta} + \delta\theta, \|\mathbf{W}_\theta \delta\theta\|_p \leq 1\} \tag{7}$$

$$\varepsilon_u = \{u: u = \hat{u} + \delta u, \|\mathbf{W}_u \delta u\|_p \leq 1\} \tag{8}$$

where $\mathbf{W}_\theta$ and $\mathbf{W}_u$ are specified positive definite weighting matrices with dimension $(n \times n)$ and $(m \times m)$, respectively. Uncertainty description (5) can be written in the form (7) by setting $p = 2$ and $\mathbf{W}_\theta = (1/r(\alpha))\,\mathbf{V}_\theta^{-1/2}$. Equation (8) can be used to describe uncertainties of the form (6) by setting $p = \infty$, $\hat{u} = (1/2)(u_{\max} + u_{\min})$, and $\mathbf{W}_u$ as a diagonal matrix with diagonal elements defined by $W_{u,jj} = 2/(u_{\max,j} - u_{\min,j})$.

B. Worst-Case Evaluation

Define $\hat{y}$ as any nominal state or output when the system is operated under the nominal control trajectory $\hat{u}$ with the nominal model parameters $\hat{\theta}$, y as its value when control input u and parameters θ are used, and the difference $\delta y = y - \hat{y}$.

Two approaches to compute the worst-case deviation in y will be described. The first approach uses a first-order series expansion, which results in analytic expressions for the worst-case uncertainties and values, and analytic expressions for the distributions. The second approach uses a higher order series expansion, which leads to higher accuracy but with the cost of increased computational burden. The worst-case analysis technique can be used whether parameter and control implementation uncertainties are considered simultaneously or independently. To simplify the presentation only, the vectors θ and u are combined into a new vector λ

$$\lambda = \begin{bmatrix} \theta \\ u \end{bmatrix} \tag{9}$$

with nominal value

$$\hat{\lambda} = \begin{bmatrix} \hat{\theta} \\ \hat{u} \end{bmatrix} \tag{10}$$

and perturbation

$$\delta\lambda = \lambda - \hat{\lambda}. \tag{11}$$

The combined weighting matrix $\mathbf{W}_\lambda$ in this case can be expressed as an $(n + m \times n + m)$ block diagonal matrix of the form

$$\mathbf{W}_\lambda = \begin{bmatrix} \mathbf{W}_\theta & 0 \\ 0 & \mathbf{W}_u \end{bmatrix} \tag{12}$$

where $\mathbf{0}$ is the matrix of zeros of compatible dimension.

1) First-Order Series Expansion: Consider the case where the deviation in outputs δy is accurately described by a first-order expansion

$$\delta y = L\delta\lambda. \tag{13}$$

For δy differentiable in $\delta\lambda$

$$L_i = \left.\frac{\partial y}{\partial \lambda_i}\right|_{\lambda=\hat{\lambda}} \text{ with } i = 1,\ldots,n+m. \tag{14}$$

The elements of the row vector L are sensitivities, which can be computed using divided differences [4], [5], [12], [20] or by integrating the original differential-algebraic equations augmented with an additional set of differential equations known as sensitivity equations [22], [25]. These sensitivities are computed automatically by some differential-algebraic equation solvers, even for distributed parameter systems [22], [37].

The worst-case deviation is defined by

$$\delta y_{w.c.} = \max_{\|\mathbf{W}_\lambda \delta\lambda\|_p \le 1} |L\delta\lambda|. \tag{15}$$

Analytical expressions for the worst-case deviation and the worst-case uncertainties $(\delta\lambda_{w.c.})$ are [33] the following.

- For $p = 1$

$$\begin{aligned}\delta y_{w.c.} &= \left\|L\mathbf{W}_\lambda^{-1}\right\|_\infty = \max_k \left|\left(L\mathbf{W}_\lambda^{-1}\right)_k\right| \\ &= \left|\left(L\mathbf{W}_\lambda^{-1}\right)_{\bar{k}}\right| \end{aligned} \tag{16}$$

$$\delta\lambda_{w.c.} = \mathbf{W}_\lambda^{-1} v \text{ with } v_k = \begin{cases} 1, & \text{for } k = \bar{k} \\ 0, & \text{for } k \ne \bar{k}. \end{cases} \tag{17}$$

- For $p = \infty$

$$\delta y_{w.c.} = \left\|L\mathbf{W}_\lambda^{-1}\right\|_1 \tag{18}$$

$$\delta\lambda_{w.c.} = \mathbf{W}_\lambda^{-1} v \text{ with } v_k = \frac{\left(L\mathbf{W}_\lambda^{-1}\right)_k}{\left|\left(L\mathbf{W}_\lambda^{-1}\right)_k\right|}. \tag{19}$$

- For any finite $p > 1$

$$\delta y_{w.c.} == \left(\sum_{k=1}^{n+m} \left(\left|\left(L\mathbf{W}_\lambda^{-1}\right)_k\right|\right)^{p/(p-1)}\right)^{(p-1)/p} \tag{20}$$

$$\delta\lambda_{w.c.} = \mathbf{W}_\lambda^{-1} v \text{ with}$$

$$v_k = \frac{\left(\left|\left(L\mathbf{W}_\lambda^{-1}\right)_k\right|\right)^{1/(p-1)}}{\left(\sum_{k=1}^{n+m} \left(\left|\left(L\mathbf{W}_\lambda^{-1}\right)_k\right|\right)^{p/(p-1)}\right)^{1/p}} \tag{21}$$

where $(A)_k$ represents the kth element of vector A. For any p, the solution of problem (15) gives one worst-case uncertainty vector, which is not unique. For example, another solution vector is obtained by multiplying the result by minus one. While both vectors achieve the same maximum deviation $\delta y_{w.c.}$, one of the vectors is associated with a worst-case increase in y and the other with a worst-case decrease. Equation (16)–(21) are also used in the more general case when parameter and implementation uncertainties are described by different norms, or even if different norms are used on different subsets of parameter and implementation uncertainties. In this case, the worst-case deviation is the sum of the deviations computed for each subset using each of the above corresponding formulas [33].

2) Higher Order Series Expansions: The first-order series expansion gives appropriate accuracy for analysis purposes for many batch and semibatch processes. However, for some processes improved accuracy is obtained using a higher order series expansion. To illustrate the approach, first consider the following uncertainty description for the combined parameter vector λ

$$a \le \delta\lambda \le b \tag{22}$$

where the vectors a and b are defined by the upper and lower bounds on the variation of model parameters $\delta\theta$ and control trajectory δu.

Consider the case when δy is accurately described by a second-order series expansion

$$\delta y = L\delta\lambda + \delta\lambda^T \mathbf{M}\delta\lambda \tag{23}$$

where L is an $(m+n)$ row vector and $\mathbf{M}$ is an $(m+n \times m+n)$ matrix. For δy twice differentiable in $\delta\lambda$, L is given by (14), and the elements of $\mathbf{M}$ are defined by

$$\mathbf{M}_{i,j} = \left.\frac{\partial^2 y}{\partial\lambda_i \partial\lambda_j}\right|_{\lambda=\hat{\lambda}} \text{ with } i,j = 1,\ldots,n+m. \tag{24}$$

This problem cannot be solved analytically but can be rewritten in terms of the mixed structured singular value μ [33]

$$\delta y_{w.c.} = \max_{a\le\delta\lambda\le b} |\delta y| = \max_{\mu_\Delta(N)\ge h} h \tag{25}$$

where

$$\mathbf{N} = \begin{bmatrix} 0 & 0 & hw \\ h\mathbf{M} & 0 & h\mathbf{M}z \\ z^T\mathbf{M} + L & W^T & z^T\mathbf{M}z + Lz \end{bmatrix} \tag{26}$$

$$w = 0.5\,(b-a) \tag{27}$$

$$z = 0.5\,(b+a) \tag{28}$$

and the perturbation block $\Delta = \text{diag}(\Delta_r, \Delta_r, \delta_c)$, where Δ_r consists of independent real scalars and δ_c is a complex scalar [9]–[11].

Upper and lower bounds for this problem can be computed by iterative μ-computation for which software packages are available [1], [50]. The upper and lower bounds are almost always tight enough for engineering purposes. The software provides a worst-case parameter vector together with the worst-case performance, for both the parameter and control implementation uncertainties. A more efficient way to solve the problem is to use skewed-μ, which requires no more effort than required for a single μ calculation [23], [24]. Although the μ-sensitivities [8], [19] could be computed to quantify the sensitivity of μ to the numerical accuracy of L and $\mathbf{M}$, it is simpler to just verify the accuracy of the results as described in Section II-C below.

For higher order series expansion the problem is handled in similar manner [33]. The $\mathbf{N}$ and Δ matrices in this case can be constructed automatically using software for multidimensional realization [47]. First- and second-order expansion have provided sufficient accuracy for all process investigated so far; thus, higher order expansions have been unnecessary. Other Hölder norms on the uncertainties, including different norms on different sets of uncertain parameters, are handled in a similar manner using the generalized structured singular value [13]–[15].

C. Verification and/or Improvement of Estimates

In this step the worst-case analysis estimates are compared with the results obtained by a nonlinear dynamic simulation using the estimated worst-case parameter vector. If the accuracy is unacceptable for a given confidence level, then a higher order expansion is used [33].

D. Estimation of Distributions

Consider the case where the uncertainty in the parameters is described by a multivariate normal distribution

$$f(\theta) = \frac{1}{\sqrt{2\pi}\det(V_\theta)^{1/2}} \exp\left(\frac{-1}{2}\left[(\theta-\hat{\theta})^T V_\theta^{-1}(\theta-\hat{\theta})\right]\right). \tag{29}$$

This will be used to estimate the distribution of each y of interest along the entire batch run. When a first-order series expansion is used, then (13) can be used to derive a normal distribution for y

$$f(y) = \frac{1}{\sigma_y\sqrt{2\pi}} \exp\left(\frac{-(y-\hat{y})^2}{(2\sigma_y^2)}\right) \tag{30}$$

with the variance $\sigma_y^2 = LV_\theta L^T$ [5]. This distribution is a function of time since the nominal value for y and the vector of sensitivities L functions of time.

Analytical expressions for the distribution cannot be obtained for higher order series expansions. In this case, the relationship between λ and y is nonlinear and the probability distribution function must be computed numerically.

III. Case Study: Batch Crystallization

Crystallization from solution is an industrially important unit operation due to its ability to provide high purity separation. The control of the crystal size distribution can be critically important for efficient downstream operations (such as filtration or drying) and product quality (e.g., bioavailability, tablet stability, dissolution rate).

A. Process Model

In this section, a brief description of the dynamic model used in this study is presented. A detailed discussion of the model equations is available elsewhere [18], [34]. The product is KNO_3, which can be characterized by one characteristic length r. The population balance equation [45] for a batch crystallizer with one-dimensional crystal growth is

$$\frac{\partial f(r,t)}{\partial t} + \frac{\partial\{G(S,\theta_g,r)f(r,t)\}}{dr} = B(S,\theta_b) \tag{31}$$

where $f(r,t)$ is the crystal size distribution, t is time, $G(S,\theta_g,r)$ is the rate of crystal growth, $B(S,\theta_b)$ is the nucleation rate, $S = (C - C_{\text{sat}})/C_{\text{sat}}$ is the relative supersaturation, C is the solute concentration, $C_{\text{sat}} = C_{\text{sat}}(T)$ is the saturation concentration, and θ_g and θ_b are vectors of growth and nucleation kinetic parameters, respectively.

A common method for simulating characteristics of the crystal size distribution is based on moments [29], [45]. The jth moment is defined by

$$\mu_j = \int_0^\infty r^j f(r,t)dr. \tag{32}$$

These moments have physical meaning. For example, μ_0 is proportional to the total number, μ_1/μ_0 is the average length, μ_2 is proportional to the total surface area, and μ_3 is proportional to the total volume of crystals in the batch.

Assuming constant volume, the solute concentration can be obtained from the mass balance on the solution phase

$$\frac{dC}{dt} = -3\rho_c k_v G\int_0^\infty r^2 f(r,t)dr - \rho_c k_v B r_0^3 \tag{33}$$

where ρ_c is the density of the crystal, r_0 is the crystal size at nucleation, and k_v is the volumetric shape factor which is the volume of a single crystal divided by r^3. In what follows, we will also need to keep track of the crystals that are grown entirely from seed, which is described by

$$\frac{\partial f(r,t)}{\partial t} + \frac{\partial\{G(S,\theta_g,r)f(r,t)\}}{dr} = 0. \tag{34}$$

Several models for growth and nucleation kinetics have been developed and are available in the literature [26], [43], [46]. The most common kinetic models when nuclei form from existing crystals are

$$G = k_g S^g \tag{35}$$

$$B = k_b S^b \int_0^\infty r^3 f(r,t)dr \tag{36}$$

where g, k_g, b, and k_b are the kinetic parameters for growth and nucleation, respectively. In the model, the moments and concentration are defined on a per mass of solvent basis. The main outputs of interest are the moments $\mu_0,\ldots,\mu_4$, and $\mu_{\text{seed},0},\ldots,\mu_{\text{seed},3}$, where $\mu_{\text{seed},j}$ is the jth moment corresponding to the crystals grown from seed.

B. Optimal Control of the Crystallizer

The quality of crystals is mostly determined by the crystal size distribution. Most studies on the optimal control of batch crystallizers focus on computing the temperature profile that optimizes some property of the crystal size distribution. In recent studies, the problem of computing the optimal temperature profile is formulated as a nonlinear optimization problem, which is then solved using a general purpose optimization algorithm, such as sequential quadratic programming (SQP) [3], [31], [38]. A convenient way to describe the optimal temperature profile is to discretize the batch time in N intervals and consider the temperatures at every discrete time $k = 0,\ldots,N$ as the optimization variables. In this case the optimal control problem can be written as follows:

$$\underset{T(k)}{\text{optimize}}\ J \tag{37}$$

subject to

$$\begin{aligned} &T_{\min}(k) \le T(k) \le T_{\max}(k),\\ &R_{\min}(k) \le \frac{dT(k)}{dT} \le R_{\max}(k)\\ &C_{\text{final}} \le C_{\text{final,max}} \end{aligned} \tag{38}$$

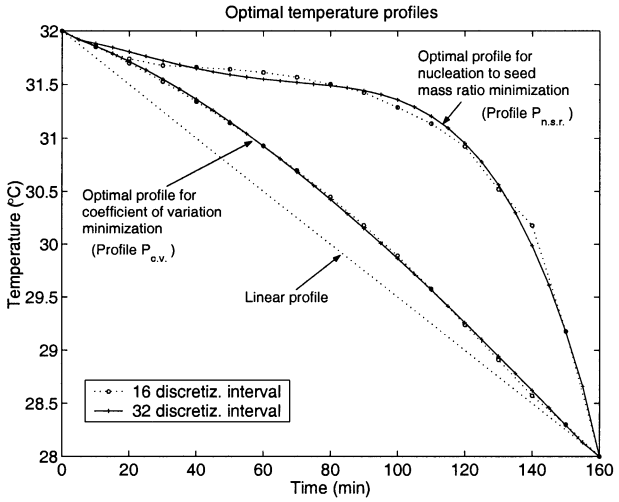

Fig. 1. Optimal cooling profiles using different levels of discretizations for performance objectives $J_{n.s.r.}$ and $J_{c.v.}$.

where $T_{\min}$, $T_{\max}$, $R_{\min}$, and $R_{\max}$ are the minimum and maximum temperatures and temperature ramp rates, respectively, during the batch. The first two constraints ensure that the temperature profile stays within the operating range of the crystallizer. The final constraint ensures that the solute concentration at the end of the batch C_{final} is smaller then a certain maximum value $C_{\text{final,max}}$ set by the minimum yield required by economic considerations. The objective J is some desired characteristic of the crystals at the end of the batch. Different objectives have been used in the literature [34], [45], [46]. In our study, the following crystal size distribution (CSD) properties were considered:

- nucleated-crystal mass to seed-crystal mass ratio

$$J_{n.s.r.} = \frac{\mu_3 - \mu_{\text{seed},3}}{\mu_{\text{seed},3}} \tag{39}$$

- coefficient of variation

$$J_{c.v.} = \sqrt{\frac{\mu_2 \mu_0}{(\mu_1)^2}} - 1 \tag{40}$$

- weight mean size

$$J_{w.m.s.} = \frac{\mu_4}{\mu_3}. \tag{41}$$

The optimization problem for $J_{n.s.r.}$ and $J_{c.v.}$ is a minimization problem, while for $J_{w.m.s}$ it is a maximization. The optimal profiles obtained for $J_{n.s.r}$ and $J_{c.v.}$ used as objectives, using different numbers of discretization points are presented in Fig. 1. For easier comparison of the results, the initial and final temperatures were fixed. Different initial temperature profiles were used to test the convergence of the SQP algorithm used to solve the optimal control problem (37) and (38). The algorithm presented very good convergence, and the optimal solution was obtained with accuracy of 10^{-9}. The optimal $J_{n.s.r.}$ and $J_{c.v.}$ obtained by implementing the resulting optimal temperature trajectories for each performance index were 8.55 and 0.81, respectively. These represent a 21.10% and 17.19% improvement, respectively, compared to the performance indexes in the case of a linear temperature profile.

The robustness of the optimal control trajectories is considered next.

TABLE I
RESULTS FOR THE WORST-CASE ANALYSIS FOR PARAMETER UNCERTAINTY USING FIRST-ORDER SERIES EXPANSION AND OPTIMAL PROFILE $P_{n.s.r.}$

Parameter	$\delta\theta_{w.c.}$				$\delta y_{w.c.}$ (%)	$(\delta y_{w.c.})_{model}$ (%)
	g	$\ln(k_g)$	b	$\ln(k_b)$		
μ_0	-0.037	-0.135	-1.135	-5.271	60.84	44.30
μ_1	-0.038	-0.139	-1.137	-5.283	43.93	35.51
μ_2	-0.039	-0.143	-1.138	-5.284	20.67	18.71
μ_3	-0.091	-0.382	-1.132	-5.267	0.68	0.68
μ_4	0.030	0.105	1.108	5.138	12.21	12.64
C	0.091	0.382	1.132	5.267	0.10	0.10
$\mu_{seed,1}$	0.016	0.048	0.995	4.594	3.56	3.60
$\mu_{seed,2}$	0.016	0.048	0.995	4.594	7.13	7.28
$\mu_{seed,3}$	0.016	0.048	0.995	4.594	10.69	11.02
$J_{n.s.r.}$	-0.021	-0.069	-1.017	-4.695	12.54	11.74
$J_{c.v.}$	0.042	0.157	1.150	5.353	6.20	6.31
$J_{w.m.s.}$	0.033	0.121	1.116	5.179	12.81	13.27

TABLE II
RESULTS FOR THE WORST-CASE ANALYSIS FOR PARAMETER UNCERTAINTY USING FIRST-ORDER SERIES EXPANSION AND OPTIMAL PROFILE $P_{c.v.}$

Parameter	$\delta\theta_{w.c.}$				$\delta y_{w.c.}$ (%)	$(\delta y_{w.c.})_{model}$ (%)
	g	$\ln(k_g)$	b	$\ln(k_b)$		
μ_0	-0.040	-0.147	-1.144	-5.319	105.35	54.82
μ_1	-0.039	-0.144	-1.138	-5.288	42.08	30.58
μ_2	-0.036	-0.135	-1.114	-5.168	10.94	9.83
μ_3	-0.138	-0.609	-0.860	-4.016	0.23	0.23
μ_4	-0.064	-0.261	-0.560	-2.674	2.90	2.92
C	0.138	0.609	0.860	4.016	0.03	0.03
$\mu_{seed,1}$	-0.062	-0.245	-1.075	-5.036	3.90	3.95
$\mu_{seed,2}$	-0.062	-0.245	-1.075	-5.036	7.80	7.98
$\mu_{seed,3}$	-0.062	-0.245	-1.075	-5.036	11.69	12.09
$J_{n.s.r.}$	0.060	0.236	1.072	5.024	12.73	12.30
$J_{c.v.}$	-0.041	-0.151	-1.148	-5.343	37.75	40.53
$J_{w.m.s.}$	-0.055	-0.222	-0.512	-2.452	2.79	2.81

C. Robustness Analysis for the Optimal Control Trajectories With Parameter Uncertainties

The nominal kinetic parameter vector used in this study is

$$\hat{\theta} = [g, \ln(k_g), b, \ln(k_b)]^T \tag{42}$$

with the nominal values: $g = 1.31$, $k_g = \exp(8.79)\ \mu\text{m}/\min$, $b = 1.84$ and $k_b = \exp(17.38)\ \text{particles}/\text{cm}^3/\min$ [18], [38]. We consider an ellipsoidal parametric uncertainty description of the form (5), characterized by the covariance matrix [34]

$$V_\theta^{-1} = \begin{bmatrix} 102\,873 & -21\,960 & -7509 & 1445 \\ -21\,960 & 4714 & 1809 & -354 \\ -7509 & 1809 & 24\,225 & -5198 \\ 1445 & -354 & -5198 & 1116 \end{bmatrix}. \tag{43}$$

Using the 2-norm ($p = 2$) and setting $\mathbf{W}_\theta = 1/r(\alpha) \cdot \mathbf{V}_\theta^{-1/2}$, the worst-case variation in y and the worst-case parameter vector for the first-order series expansion can be derived from (20) and (21):

$$\delta y_{w.c.} = r(\alpha) \left(L V_\theta L^T\right)^{1/2} \tag{44}$$

$$\delta\theta_{w.c.} = \frac{r(\alpha)}{\left(L V_\theta L^T\right)^{1/2}} V_\theta L^T. \tag{45}$$

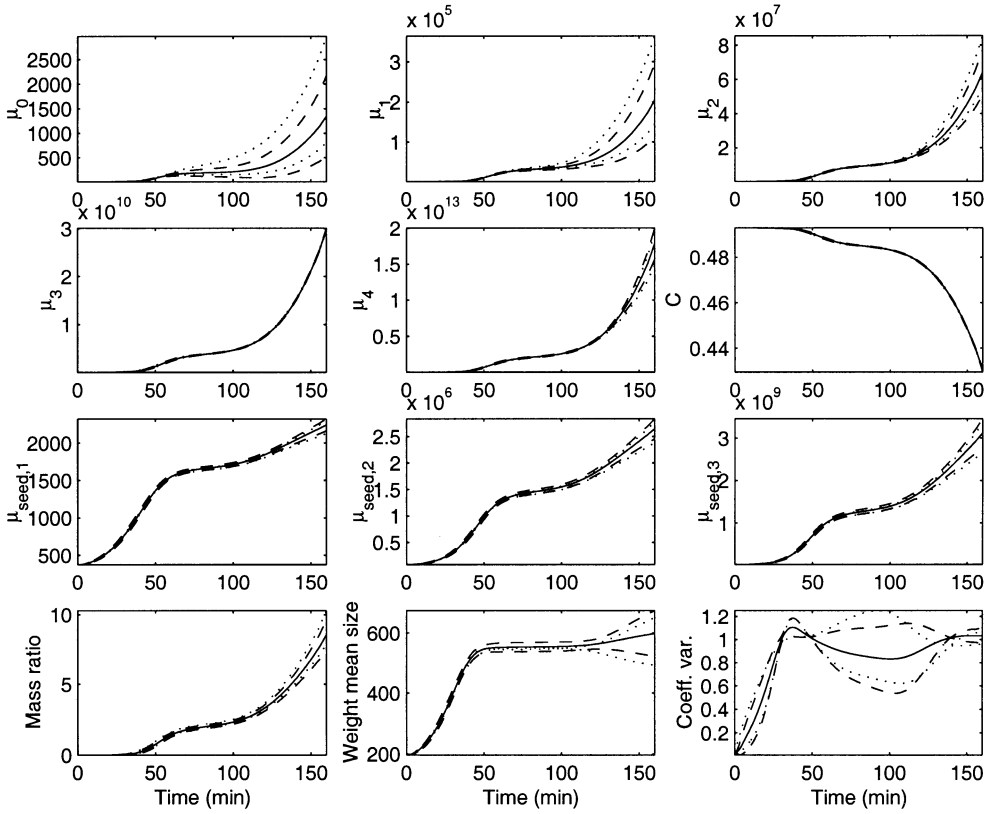

Fig. 2. Comparison between results of the first-order worst-case analysis for $\alpha = 0.95$, and the dynamic simulation during the whole batch for profile $P_{n.s.r.}$ (solid line is the nominal value; doted line is $y_{w.c.}$ for $\delta\theta_{w.c.}$ and $-\delta\theta_{w.c.}$, respectively; and dashed line is $y_{w.c}$ obtained from the dynamic simulation $\delta\theta_{w.c.}$ and $-\delta\theta_{w.c.}$, respectively).

These expressions are applied at each time t, using the sensitivity vector at the corresponding time, $L(t)$, which was computed by simultaneous solution of the model equations augmented with the sensitivity equations. The accuracy of the sensitivity coefficients was verified with the finite difference method using the centered difference approximation with different but properly scaled steps ε, which gives an accuracy of $O(\varepsilon^2)$.

The worst-case analysis has been performed for the solute concentration, the moments, and the three CSD properties. The results for the confidence region $\alpha = 0.95$ are presented in Table I for the temperature profile $P_{n.s.r.}$ and in Table II for the profile $P_{c.v.}$, respectively. Tables I and II show that the nucleation to seed mass ratio is sensitive to parameter uncertainties in both profiles (12% variation). Parameter uncertainties have very different effects on the coefficient of variation and weight mean size for the two optimal control trajectories. The weight mean size is sensitive to parameter uncertainties for Profile $P_{n.s.r.}$, but is not sensitive for Profile $P_{c.v.}$. The coefficient of variation is very sensitive to parameter uncertainties for the temperature profile that minimizes the coefficient of variation $(P_{c.v.})$, but is not nearly as sensitive for the profile that minimizes the nucleated crystal mass to seed crystal mass ratio $(P_{n.s.r.})$. This supports the well-known fact that control trajectories that optimize a particular nominal performance objective can be much more sensitive to parameter uncertainties than other control trajectories. In other words, there can be a tradeoff between nominal performance and robustness.

The moments μ_0 and μ_1 show significant sensitivity to parameter uncertainties. Also note that the worst case parameter vectors are identical for μ_3 and C (modulo sign), and for $\mu_{\text{seed},1}$, $\mu_{\text{seed},2}$, and $\mu_{\text{seed},3}$. The effect of parameter uncertainty decreases from μ_0 to μ_3 and increases from $\mu_{\text{seed},1}$ to $\mu_{\text{seed},3}$. In physical terms, this means that parameter uncertainty has a much larger effect on the total length of crystals than on the total length of the crystals grown from seed. This implies that the parameter uncertainty greatly affects the total length of the crystals grown from nuclei. These results also imply that the parameter uncertainty has a large effect on the total volume of crystals grown from seed, while having a small effect on the total volume of crystals. This implies that the parameter uncertainty has a strong effect on the relative volume of crystals grown from seed and crystals grown from nuclei, although the effect on the total volume of all crystals is negligible.

Figs. 2 and 3 depict the upper and lower bounds along the whole batch, obtained using the first-order technique as well as the dynamic simulation for the worst-case parameter vectors from Tables I and II, respectively. It can be seen that first-order series expansion gives satisfactory qualitative results that are also reasonably quantitative for all parameters except moments μ_0 and μ_1. For these parameters, the errors are significantly larger at the end of the batch (see Tables I and II). For the rest of the parameters, the accuracy of the first-order expansion is within two significant figures (or close to it) for the whole batch run. Consequently, the first-order series expansion can

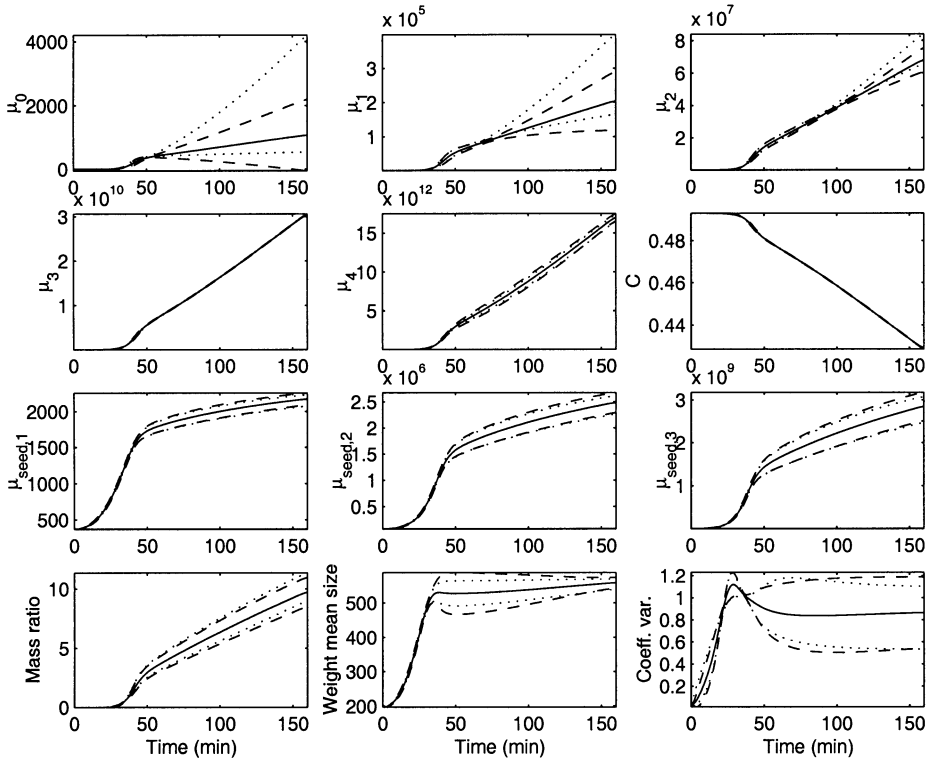

Fig. 3. Comparison between results of the first-order worst-case analysis for $\alpha = 0.95$, and the dynamic simulation during the whole batch for profile $P_{c.v.}$ (solid line is the nominal value; dotted line is $y_{w.c.}$ for $\delta\theta_{w.c.}$ and $-\delta\theta_{w.c.}$, respectively; and dashed line is $y_{w.c}$ obtained from the dynamic simulation $\delta\theta_{w.c.}$ and $-\delta\theta_{w.c.}$, respectively).

lead to satisfactory accuracy for engineering purposes, however in some cases a higher order expansion may be desired to increase accuracy.

All moments except for μ_3 show increasing sensitivity to parameter uncertainty during the batch. The effect of uncertainties is large enough that feedback control techniques, such as nonlinear model predictive control (NMPC), should be considered for suppressing the effect of parameter uncertainty. Parameter uncertainty has interesting effects on the weight mean size and coefficient of variation during the batch for the different temperature profiles (see Figs. 2 and 3). In the case of profile $P_{n.s.r.}$, the weight mean size shows small sensitivity to parameter uncertainty for the first three quarters of the batch; then, the sensitivity increases suddenly, reaching almost 13% at the end (see Table I). The coefficient of variation presents very high sensitivity during the middle of the batch and much lower sensitivity at the beginning and end of the batch. For this CSD parameter, two minimum sensitivity points can also be observed: one at 50 min and the second at 140 min. From this analysis, the sensitivity of the coefficient of variation to parameter uncertainty for profile $P_{n.s.r.}$ can be reduced by stopping the batch at 140 min, when all the CSD parameters and moments have lower sensitivity. However, this would result in a higher solute concentration at the end of the batch, thus a smaller yield for the crystallizer.

When the analysis is performed using optimal trajectory $P_{c.v.}$, a different behavior is observed. The weight mean size reaches a maximum sensitivity to parameter uncertainty at 50 min (see Fig. 3), and then decreases continuously arriving at

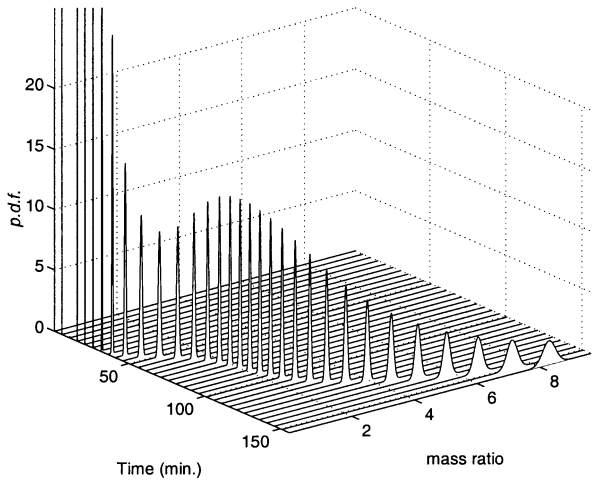

Fig. 4. Mass ratio distributions for optimal temperature trajectory $P_{n.s.r.}$.

a deviation of less than 3% at the end of the batch (see Table II). The coefficient of variation has high sensitivity to parameter uncertainty by the middle of the batch, and the worst-case deviation is roughly constant until the end of the batch.

When many confidence levels are considered, then the worst-case y is a function of the confidence level α and time t. The worst-case analysis can be performed for any $\alpha \in (0, 1)$ over the entire batch run. While this approach can be useful, it can be more informative to plot the distribution function for each y as a function of time. The distribution function is estimated from the analytical expression (30). The resulting

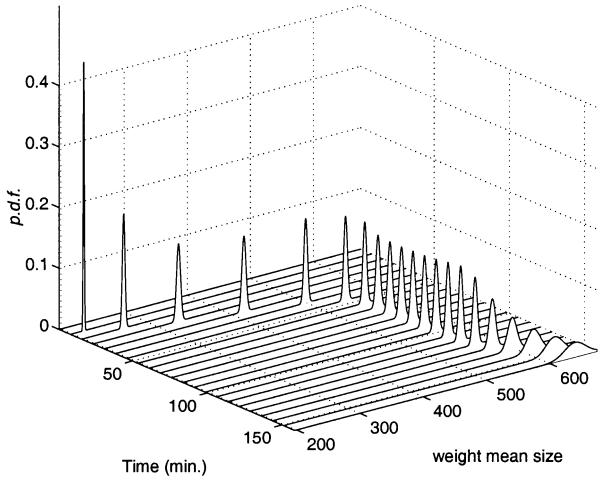

Fig. 5. Weight mean size distributions for optimal temperature trajectory $P_{n.s.r.}$.

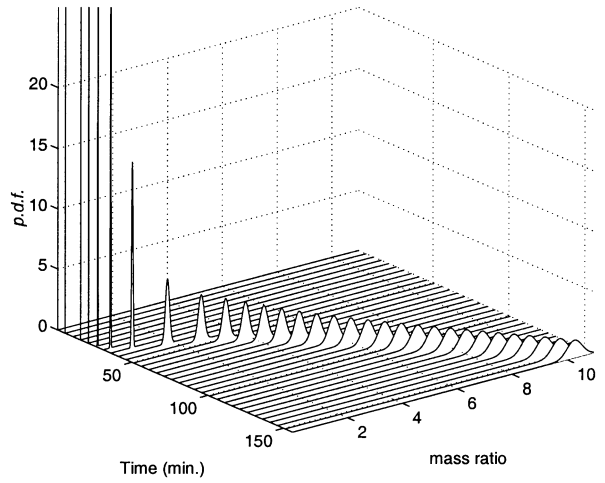

Fig. 6. Mass ratio for optimal temperature trajectory $P_{c.v.}$.

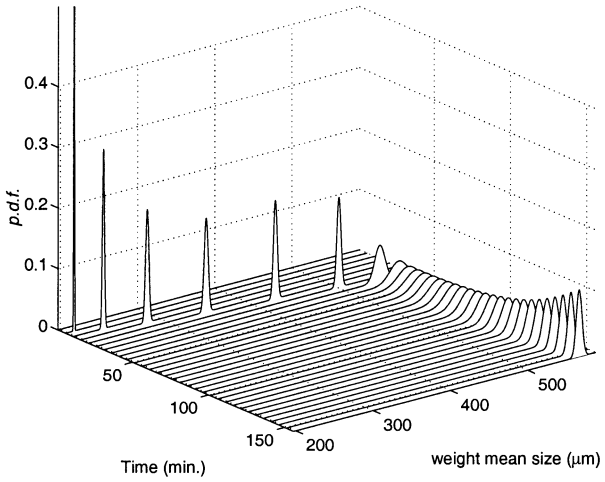

Fig. 7. Weight mean size distribution for optimal temperature trajectory $P_{c.v.}$.

distribution plots show the distribution functions along the whole batch. The distribution plots for the CSD parameters $J_{n.s.r.}$ and $J_{w.m.s.}$ are shown in Figs. 4 and 5 for the optimal trajectory $P_{n.s.r.}$, and in Figs. 6 and 7 for temperature profile $P_{c.v.}$, respectively. Figs. 4–7 show how the distributions of the CSD parameters vary during the batch for the probability distribution for the model parameters. These figures provide a richer intuitive feeling for the effect of parameter uncertainties than the worst-case values reported for a single confidence level, as in Tables I and II and Figs. 2 and 3. These distributions provide a stochastic representation for the effect of parameter uncertainties, as opposed to the worst-case representation given in Figs. 2 and 3.

TABLE III
RESULTS FOR THE WORST-CASE ANALYSIS, USING FIRST-ORDER SERIES EXPANSION, FOR IMPLEMENTATION UNCERTAINTY OF OPTIMAL PROFILE $P_{n.s.r.}$

Parameter	$\bar{k}$	±0.1 °C		±0.5 °C	
		$\delta y_{w.c.}$ (%)	$(\delta y_{w.c.})_{model}$ (%)	$\delta y_{w.c.}$ (%)	$(\delta y_{w.c.})_{model}$ (%)
μ_0	31	3.42	3.52	17.10	18.75
μ_1	28	3.05	3.14	15.27	16.69
μ_2	10	2.80	2.88	14.00	15.88
μ_3	10	2.54	2.60	12.72	14.34
μ_4	16	3.06	3.16	15.29	17.63
C	10	0.37	0.37	1.86	1.90
$\mu_{seed,1}$	6	1.12	1.13	5.62	5.99
$\mu_{seed,2}$	6	2.25	2.30	11.25	12.74
$\mu_{seed,3}$	6	3.37	3.49	16.87	20.26
$J_{n.s.r.}$	6	6.60	7.02	32.98	42.54
$J_{c.v.}$	16	0.92	0.93	4.62	4.85
$J_{w.m.s.}$	8	1.91	1.95	9.55	10.56

TABLE IV
RESULTS FOR THE WORST-CASE ANALYSIS, USING FIRST-ORDER SERIES EXPANSION, FOR IMPLEMENTATION UNCERTAINTY OF OPTIMAL PROFILE $P_{c.v.}$

Parameter	$\bar{k}$	±0.1 °C		±0.5 °C	
		$\delta y_{w.c.}$ (%)	$(\delta y_{w.c.})_{model}$ (%)	$\delta y_{w.c.}$ (%)	$(\delta y_{w.c.})_{model}$ (%)
μ_0	9	2.82	2.89	14.10	15.74
μ_1	8	4.05	4.19	20.27	23.66
μ_2	8	3.73	3.86	18.64	21.69
μ_3	8	2.44	2.50	12.19	13.67
μ_4	1	3.15	3.15	15.74	16.56
C	8	0.37	0.37	1.83	1.86
$\mu_{seed,1}$	5	0.50	0.50	2.51	2.60
$\mu_{seed,2}$	5	1.00	1.02	5.01	5.41
$\mu_{seed,3}$	5	1.50	1.53	7.52	8.42
$J_{n.s.r.}$	5	4.34	4.50	21.69	25.23
$J_{c.v.}$	8	2.11	2.16	10.54	11.97
$J_{w.m.s.}$	7	1.54	1.57	7.72	8.48

D. Worst-Case Analysis of the Effect of Implementation Uncertainties on Optimal Control Trajectories

Now, consider control implementation uncertainties represented by independent bounds on each temperature at each discretization point. Thirty-two discretization intervals were used, which results in 33 values for the temperature along the control trajectory. The objective of this analysis is to compute how the moments and CSD properties are effected by implementation uncertainties for the optimal control trajectory at a certain moment of the batch. This can be achieved by using the vector ∞-norm, in which case (18) and (19) are used to perform the analysis.

TABLE V
RESULTS FOR THE WORST-CASE ANALYSIS, USING SECOND-ORDER SERIES EXPANSION, FOR IMPLEMENTATION UNCERTAINTY OF $\pm 0.5^{\circ}$C OF OPTIMAL PROFILE $P_{n.s.r}$

$\delta y_{w.c.}$ (%)											
μ_0	μ_1	μ_2	μ_3	μ_4	C	$\mu_{seed,1}$	$\mu_{seed,2}$	$\mu_{seed,3}$	$J_{n.s.r.}$	$J_{c.v.}$	$J_{w.m.s.}$
17.9	17.2	16.5	13.4	16.8	1.9	6.3	13.3	18.4	37.26	4.9	11.2

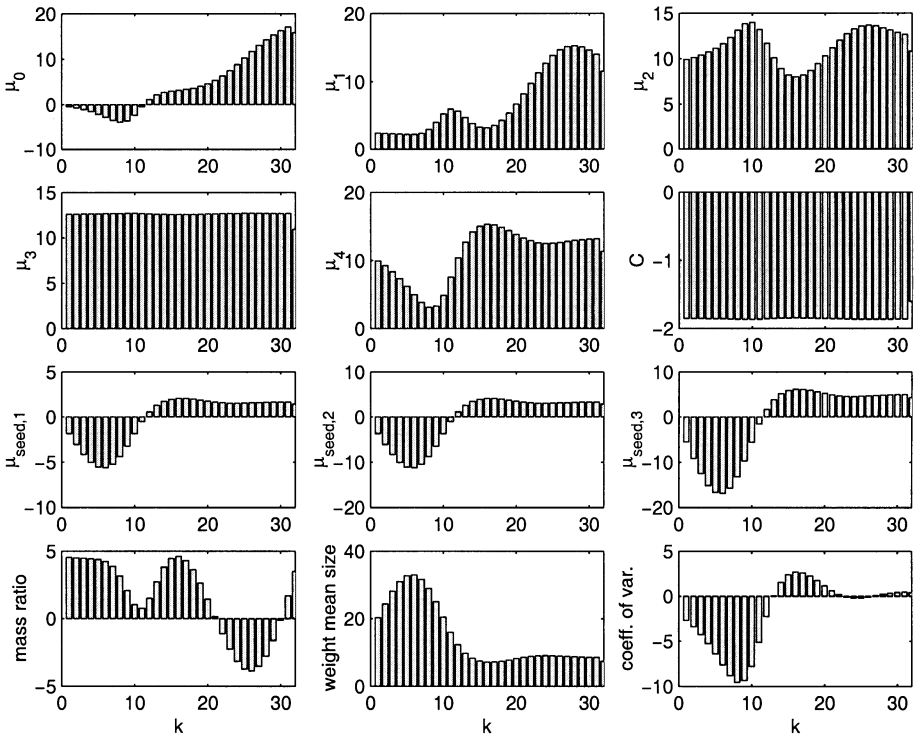

Fig. 8. Sensitivity of states and CSD parameters (in percent) at the end of the batch to 0.5°C variation of the kth temperature value from the discrete optimal control trajectory $P_{n.s.r.}$.

The first-order analysis results for implementation uncertainties of $\pm$ 0.5 °C and $\pm$ 0.1 °C for the optimal control trajectories $P_{n.s.r.}$ and $P_{c.v.}$ are summarized in Tables III and IV, respectively. These tables show the time index k for the most significant temperature in the optimal control trajectory, denoted by $\bar{k}$, the worst-case degradation of the moments and CSD properties at the end of the batch, as well as the relative error of the worst-case estimates compared to the values obtained from dynamic simulation. The nucleation to seed mass ratio is the most sensitive to control implementation uncertainties, showing significant degradation for even 0.1 °C variation of a single temperature, indicated by $\bar{k}$. All the other variables show a relatively low sensitivity to a variation of 0.1 °C, while most variables are significantly sensitive to 0.5 °C variations from the optimal temperature trajectory. The relative errors from Tables III and IV show that the first-order series expansion gives good accuracy if the temperature variations are of 0.1 °C or smaller. However, the accuracy of the first-order series expansion is reduced when the control implementation uncertainty increases, which motivates the use of a second-order series expansion. The relative errors using the second-order series expansion are presented in Table V. The second-order approach gave very tight upper and lower bounds on the worst-case values (with a relative difference smaller than 0.5%), leading to significant improvement of the accuracy. However, the first-order series expansion produces results that are accurate enough for engineering purposes.

The approach can be used to compute the effect of uncertainty in each temperature from the discrete optimal control trajectory, on all states and CSD properties. The results can be used to determine the period of the batch control implementation uncertainties that has the most important effect on a certain process variable y at the end of the batch. The results obtained for optimal control trajectories $P_{n.s.r.}$ and $P_{c.v.}$, are shown in Figs. 8 and 9, respectively. From this analysis, it can be observed that implementation uncertainties have the greatest effect in the first third of the batch for most of the states and all of the CSD properties (exceptions are μ_0 and μ_1). For example, while a deviation with 0.5 °C from trajectory $P_{n.s.r.}$ in any temperature for $k \geq 12$ causes a variation of the weight mean size at the end of the batch within 10%, a 0.5 °C variation in any temperature for $k \leq 11$ results in 20–30% variation in the weight mean size. Consequently, the implementation of a feedback control algorithm capable of high accuracy tracking

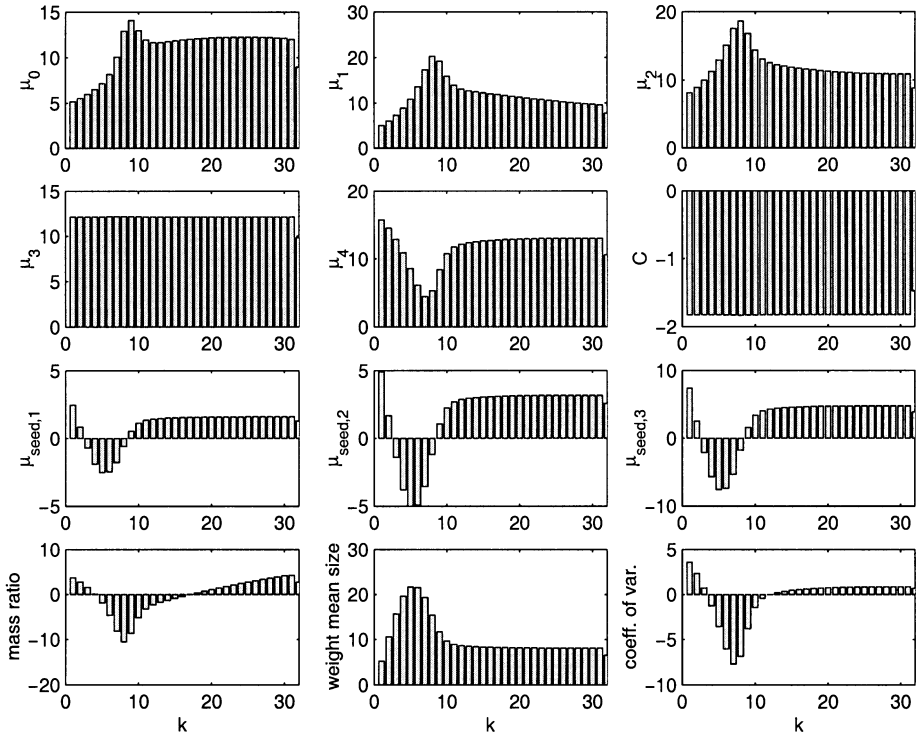

Fig. 9. Sensitivity of states and CSD parameters (in percent) at the end of the batch to 0.5 °C variation of the kth temperature value from the discrete optimal control trajectory $P_{c.v.}$.

of the temperature profile is of increased importance in the first third of the batch run, for most process variables. The low-order moments μ_0 and μ_1 at the end of the batch run are most sensitive to deviations in the control trajectory in the last quarter of the batch run. This agrees with physical intuition, in that the optimal control trajectory $P_{n.s.r.}$ has a rapid drop in temperature in the last quarter of the batch run, resulting in significant nucleation. Small deviations in the temperature in the last quarter of the batch is expected to significantly affect the amount of nucleation and has a large effect on the lower order moments at the end of the batch.

IV. Conclusion

An approach was proposed to estimate the effect of parameter and control implementation uncertainties on finite-time control trajectories, which are used in batch and semibatch optimal control problems. The approach can compute the worst-case deviations of the state variables and product properties along the whole trajectory. The technique also determines the part of the control trajectory which is most effected by implementation inaccuracies, in terms of the effect on states or product properties. Also, a method was given to estimate the distributions of the states and outputs along the entire control trajectory. The algorithms are applicable for nonlinear lumped and distributed parameter systems. The robustness analysis approach was applied to a batch crystallization process, to quantify the effects of uncertainties in nucleation and growth kinetics, and on uncertainties in the implementation of optimal temperature trajectories.

References

[1] G. J. Balas, J. C. Doyle, K. Glover, A. K. Packard, and R. S. R. Smith, *μ-Analysis and Synthesis Toolbox (μ-Tools): Matlab Functions for the Analysis and Design of Robust Control Systems*. Natick, MA: The MathWorks, Inc., 1992.

[2] M. D. Barrera and L. B. Evans, "Optimal design and operation of batch processes," *Chem. Eng. Comm.*, vol. 82, pp. 45–66, 1989.

[3] P. I. Barton, R. J. Allgor, W. F. Feehery, and S. Galan, "Dynamic optimization in a discontinuous world," *Ind. Eng. Chem. Res.*, vol. 37, pp. 966–981, 1998.

[4] D. M. Bates and D. G. Watts, *Nonlinear Regression Analysis and Its Applications*. New York: Wiley, 1988.

[5] J. V. Beck and K. J. Arnold, *Parameter Estimation in Engineering and Science*. New York: Wiley, 1977.

[6] L. T. Beigler, I. E. Grossmann, and A. W. Westerberg, *Systematic Methods of Chemical Process Design*. Upper Saddle River, NJ: Prentice-Hall, 1997.

[7] R. D. Braatz and O. D. Crisalle, "Robustness analysis for systems with ellipsoidal uncertainty," *Int. J. Robust Nonlinear Contr.*, vol. 8, pp. 1113–1117, 1998.

[8] R. D. Braatz and M. Morari, "Sensitivities as an aid for robust identification," in *Proc. Amer. Contr. Conf.*, vol. 1, 1991, pp. 231–236.

[9] R. D. Braatz and E. L. Russell, "Robustness margin computation for large scale systems," *Comput. Chem. Eng.*, vol. 23, pp. 1021–1030, 1999.

[10] R. D. Braatz, P. M. Young, J. C. Doyle, and M. Morari, "Computational complexity of μ calculation," in *Proc. Amer. Contr. Conf.*, 1993, pp. 1682–1683.

[11] ——, "Computational complexity of μ calculation," *IEEE Trans. Automat. Contr.*, vol. 39, pp. 1000–1002, May 1994.

[12] M. Caracotsios and W. E. Stewart, "Sensitivity analysis of initial value problems with mixed ODE's and algebraic equations," *Comput. Chem. Eng.*, vol. 9, pp. 359–365, 1985.

[13] V. -S. Chellaboina, W. M. Haddad, and D. S. Bernstein, "Structured matrix norms for robust stability and performance with block-structured uncertainty," *Int. J. Contr.*, vol. 71, pp. 535–557, 1998.

[14] J. Chen, M. K. H. Fan, and C. N. Nett, "Structured singular values and stability analysis of uncertain polynomials, Part 1: The generalized μ," *Syst. Contr. Lett.*, vol. 23, pp. 53–65, 1994.

[15] ——, "Structured singular values and stability analysis of uncertain polynomials, Part 2: A missing link," *Syst. Contr. Lett.*, vol. 23, pp. 97–109, 1994.
[16] S. H. Chung, D. L. Ma, and R. D. Braatz, "Optimal seeding in batch crystallization," *Can. J. Chem. Eng.*, vol. 77, pp. 590–596, 1999.
[17] ——, "Optimal model-based experimental design in batch crystallization," *Chemometrics Intell. Lab. Syst.*, vol. 50, pp. 83–90, 2000.
[18] S. H. Chung and R. D. Braatz, "Modeling and Simulation of Crystallization," Univ.f Illinois, Urbana, IL, LSSRL Tech. Memo UIUC-LSSRL 98-004, 1998.
[19] J. Douglas and M. Athans, "The calculation of μ-sensitivities," in *Proc. Amer. Contr. Conf.*, vol. 1, 1995, pp. 437–441.
[20] A. H. Evers, "Sensitivity analysis in dynamic optimization," *J. Optimi. Theory Applicat.*, vol. 32, pp. 17–37, 1980.
[21] M. K. H. Fan, A. L. Tits, and J. C. Doyle, "Robustness in the presence of mixed parametric uncertainty and unmodeled dynamics," *IEEE Trans. Automat. Contr.*, vol. 36, pp. 25–38, Jan. 1991.
[22] W. F. Feehery, J. E. Tolsma, and P. I. Barton, "Efficient sensitivity analysis of large-scale differential-algebraic systems," *Appl. Numer. Math.*, vol. 25, pp. 41–54, 1997.
[23] G. Ferreres and V. Fromion, "Computation of the robustness margin with the skewed μ tool," *Syst. Contr. Lett.*, vol. 32, pp. 193–202, 1997.
[24] ——, "A new upper bound for the skewed structured singular value," *Int. J. Robust Nonlinear Contr.*, vol. 9, pp. 33–49, 1999.
[25] S. Galan, W. F. Feehery, and P. I. Barton, "Parameter sensitivity functions for hybrid discrete-continuous systems," *Appl. Numer. Math.*, vol. 31, pp. 17–48, 1999.
[26] J. Garside, "Advances in characterization of crystal growth," in *Advances in Crystallization From Solutions*, vol. 80, AIChE Symposium Series no. 240, New York, 1984, AIChE, pp. 23–38.
[27] G. Gattu and E. Zafiriou, "A methodology for on-line setpoint modification for batch reactor control in the presence of modeling error," *Chem. Eng. J.*, vol. 75, pp. 21–29, 1999.
[28] H. Golub and F. van Loan, *Matrix Computations*. Baltimore, MD: Johns Hopkins Univ. Press, 1983.
[29] H. M. Hulbert and S. Katz, "Some problems in particle technology," *Chem Eng. Sci.*, vol. 19, p. 555, 1964.
[30] E. Kreindler, "On performance sensitivity of optimal control problems," *Int. J. Contr.*, vol. 15, pp. 481–486, 1972.
[31] Y. D. Lang, A. M. Cervantes, and L. T. Biegler, "Dynamic optimization of a batch cooling crystallization process," *Ind. Eng. Chem. Res.*, vol. 38, pp. 1469–1477, 1999.
[32] L. Ljung, *System Identification: Theory for the User*. Englewood Cliffs, NJ: Prentice-Hall, 1987.
[33] D. L. Ma and R. D. Braatz, "Worst-case analysis of finite-time control policies," *IEEE Trans. Contr. Syst. Technol.*, vol. 9, pp. 766–774, Sept. 2001.
[34] D. L. Ma, S. H. Chung, and R. D. Braatz, "Worst-case performance analysis of optimal batch control trajectories," *AIChE J.*, vol. 45, pp. 1469–1476, 1999.
[35] ——, "Worst-case analysis of batch and semibatch control trajectories," presented at the AIChE Annual Meet., Dallas, TX, 1999, Paper 10A07.
[36] ——, "Worst-case performance analysis of optimal batch control trajectories," in Proc. European Contr. Conf., Germany, Aug.–Sept. 1999, IFAC, Paper F1011-2.
[37] T. Maly and L. Petzold, "Numerical methods and software for sensitivity analysis of differential-algebraic systems," *Appl. Numer. Math.*, vol. 20, pp. 57–79, 1996.
[38] S. M. Miller and J. B. Rawlings, "Model identification and control strategies for batch cooling crystallizers," *AIChE J.*, vol. 40, pp. 1312–1327, 1994.
[39] M. Morari and E. Zafiriou, *Robust Process Control*. Englewood Cliffs, NJ: Prentice-Hall, 1989.
[40] Z. Nagy and S. Agachi, "Productivity optimization of the PVC batch suspension reactor using genetic algorithm," in *Proc. 2nd Conf. Process Integration, Modeling, Optimization Energy Saving Pollution Reduction*, Budapest, Hungary, 1999, pp. 487–492.
[41] ——, "Model predictive control of a PVC batch reactor," *Comput. Chem. Eng.*, vol. 21, no. 6, pp. 571–591, 1997.
[42] M. Nikolaou and V. Manousiouthakis, "Robust control of batch processes," in *Proc. American Control Conf.*, Piscataway, NJ, 1988, pp. 665–670.
[43] J. Nyvlt, O. Sohnel, M. Matuchova, and M. Broul, *The Kinetics of Industrial Crystallization*. Amsterdam, The Netherlands: Elsevier, 1985, vol. 19, Chem. Eng. Monographs.
[44] D. W. Peterson, "On sensitivity in optimal control problems," *J. Optimization Theory Applicat.*, vol. 13, pp. 56–73, 1974.
[45] A. Randolph and M. A. Larson, *Theory of Particulate Process*, 2nd ed. San Diego, CA: Academic, 1988.
[46] J. B. Rawlings, S. M. Miller, and W. R. Witkowski, "Model identification and control of solution crystallization processes: A review," *Ind. Eng. Chem. Res.*, vol. 32, pp. 1275–1296, 1993.
[47] E. L. Russell, C. P. H. Power, and R. D. Braatz, "Multidimensional realizations of large scale uncertain systems for multivariable stability margin computation," *Int. J. Robust Nonlinear Contr.*, vol. 7, pp. 113–125, 1997.
[48] T. Togkalidou and R. D. Braatz, "A bilinear matrix inequality approach to the robust nonlinear control of chemical processes," in *Proc. American Control Conf.*, 2000, pp. 1732–1736.
[49] P. M. Young, "Robustness analysis with full-structured uncertainties," *Automatica*, vol. 33, pp. 2131–2145, 1997.
[50] P. M. Young, M. P. Newlin, and J. C. Doyle, "Practical computation of the mixed μ problem," in *Proc. American Control Conf.*, 1992, pp. 2190–2194.
[51] K. Zhou and J. C. Doyle, *Robust and Optimal Control*. Englewood Cliffs, NJ: Prentice-Hall, 1992.

Zoltán K. Nagy received the M.S. and Ph.D. degrees in chemical engineering from the Babes-Bolyai University, Cluj, Romania, in 1995 and 2001, respectively.

Since 1995, he has been with the Chemical Engineering Department at the same university where he currently holds a faculty position. In 1996, he was Visiting Professor at the University of the South, Sewanee, TN. In 1997, he worked as Honorary Research Assistant at the University of Liverpool, Liverpool, U.K. Between 1997 and 2000, he has worked as Research Associate in different international research teams on various process control projects. He is currently a Research Associate at the University of Illinois at Urbana-Champaign, Urbana. His research interests include modeling and control of chemical processes, virtual instrumentation and process monitoring.

Dr. Nagy received a Tempus Research Award in 1997 and an NSF-NATO postdoctoral research award in 2001.

Richard D. Braatz received the Ph.D. degree from the California Institute of Technology, Pasadena, in 1993.

He spent a postdoctoral year at DuPont studying various control systems problems including polymer film extrusion control. Currently, he is a Professor at the University of Illinois, Urbana-Champaign. He is co-author of the books *Data-driven Techniques for Fault Detection and Diagnosis in Chemical Processes* (London, U.K.: Springer-Verlag, 2000), *Identification and Control of Sheet and Film Processes* (London, U.K.: Springer-Verlag, 2000), and *Fault Detection and Diagnosis in Industrial Systems* (London, U.K.: Springer-Verlag, 2001). His research is in the modeling and control of complex chemical processes including pharmaceutical crystallization, microelectronics processes, and sheet and film processes.

Dr. Braatz received the Hertz Doctoral Thesis Prize, the DuPont Young Faculty Award, the Xerox Award for Faculty Research, and the Donald P. Eckman Award of the American Automatic Control Council. In 2001, he gave a Plenary Lecture at the American Control Conference and delivered the Ernest W. Thiele Lecture at the University of Notre Dame.